

# Technical Evaluation of Engineering Model of Ultra-Small Transmitter Mounted on Sweetpotato Hornworm

Isao Nakajima<sup>1\*</sup>, Yoshiya Muraki<sup>1</sup>, Kokuryo Mitsushashi<sup>1</sup>,  
Hiroshi Juzoji<sup>2</sup>, Yukako Yagi<sup>3</sup>

## Abstract

The authors are making a prototype flexible board of a radio-frequency transmitter for measuring an electromyogram (EMG) of a flying moth and plan to apply for an experimental station license from the Ministry of Internal Affairs and Communications of Japan in the summer of 2022. The goal is to create a continuous low-dose exposure standard that incorporates scientific and physiological functional assessments to replace the current standard based on lethal dose 50. This paper describes the technical evaluation of the hardware. The signal of a bipolar EMG electrode is amplified by an operational amplifier. This potential is added to a voltage-controlled crystal oscillator (27 MHz, bandwidth: 4 kHz), frequency-converted, and transmitted from an antenna about 10 cm long (diameter: 0.03 mm). The power source is a 1.55-V wrist-watch battery that has a total weight of about 0.3 g (one dry battery and analog circuit) and an expected operating time of 20 minutes. The output power is  $-7$  dBm and the effective isotropic radiated power is  $-40$  dBm. The signal is received by a dual-whip antenna (2.15 dBi) at a distance of about 100 m from the moth. The link margin of the communication circuit is above 30 dB within 100 m. The concepts of this hardware and the measurement data are presented in this paper. This will be the first biological data transmission from a moth with an official license. In future, this telemetry system will improve the detection of physiological abnormalities of moths.

**Key Words:** LD50 (Lethal Dose, 50%), Low Dose Exposure, VCXO.

## I. INTRODUCTION

### 1.1. Fukushima Nuclear Power Plant Accident and *Pseudozizeeria Maja* Argia

Otaki et al. collected *Pseudozizeeria maha* in the Fukushima area in May 2011 and found relatively mild abnormalities in some of them [1]. The severity of abnormalities was higher in the F1 offspring obtained from females of the first instar. These abnormalities were inherited by the F2 generation. Experiments have shown that low-dose external and internal exposure of individuals from non-contaminated areas reproduced the same abnormalities. These results indicate that anthropogenic radionuclides from the Fukushima Nuclear Power Plant have caused morphological and genetic damage to *Pseudozizeeria maha*. However, only morphological abnormalities such as wing shape and wing pattern were recorded [2-6]. The effects on physiological function are unknown.

### 1.2. Persistent Low-Dose Exposure

Lethal dose 50 (LD50), a measure of acute toxicity, refers to the amount of pesticide or radiation that kills half of the exposed individuals. Sustained low-dose exposure to pesticides and radiation cannot be assessed simply on the basis of LD50; however, no optimal criteria have been reported. LD50 is the rate of survival, not a measure of physiological dysfunction in healthy organisms due to exposure [7-10].

This study aims to detect the impairment of motor function in insects exposed to sustained low concentrations of radiation by monitoring their physiology and detecting the impairment of flap reduction and peak-to-peak temporal fluctuations ( $\Delta t$ ). Biotelemetry can be used to transmit moth physiological data. The battery limits the amount of data that can be recorded. Nevertheless, data from moths pinned to a platform can be compared and evaluated [11-22].

Manuscript received March 10, 2022; Revised April 12, 2022; Accepted April 27, 2022. (ID No. JMIS-22M-03-007)

Corresponding Author (\*): Isao Nakajima, +81-90-8850-8380, jh1rnz@aol.com

<sup>1</sup>Nakajima Labo, Seisa University, Yokohama, Japan, jh1rnz@aol.com

<sup>2</sup>EFL Inc., Takaoka, Japan, juzoji@yahoo.co.jp

<sup>3</sup>Department of Pathology & Lab Medicine, Memorial Sloan Kettering Cancer Center, New York, NY, USA. yagi@mskcc.org

## II. PREPARATORY EXPERIMENTS

A physiological experiment was performed by hanging a moth was suspended using pins that were connected to copper wires (Fig. 1 and Fig. 2). The hawkmoth periodically contacts the muscles inside the exoskeleton, resulting in deformation of the exoskeleton and the movement of the feathers connected by the “hinge” up and down. Fig. 3 shows the anatomy of primary flight muscles those of two have a cycles: The Dorsal Ventral Muscle (DVM) contract, causing a down-strok that creates life. Therefore, electrodes are inserted into two muscle groups. The preliminary experiments were conducted as follows. We recorded a two-channel electromyogram (EMG) and the angular velocity corresponding to the pitch angle associated with wing flapping for 100 sweetpotato hawkmoths (*Agrius convolvuli*)(Fig. 4), 50 females and 50 males) with the animals suspended and constrained in air. Overall, the angular velocity and ampli-



Fig. 1. Lateral view of sweetpotato hornworm.

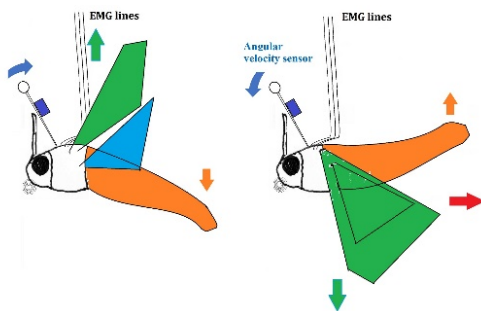


Fig. 2. Monitor of EMGs and angular velocity with pins linking copper wires.

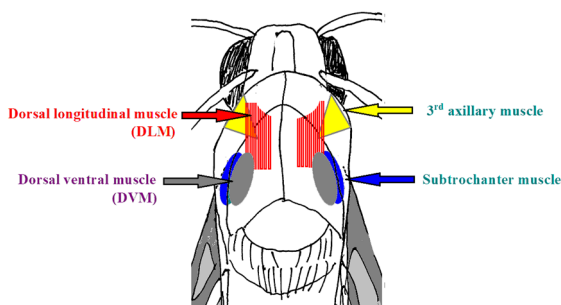


Fig. 3. Anatomy of muscles.

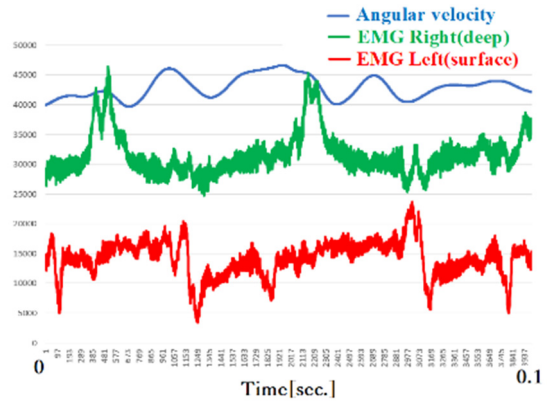


Fig. 4. Obtained EMG data and angular velocity, the muscles of DLM is green and DVM is red line.

tude of the EMG signals had a high correlation, with a correlation coefficient of  $R = 0.792$ . An analysis of the peak-to-peak EMG intervals, which correspond to the RR intervals of ECG signals, indicated a correlation between  $\Delta t$  fluctuation and angular velocity of  $R = 0.379$ . Thus, the accuracy of the regression curve was relatively poor. What is  $\Delta t$ , in other words, is the origin of the temporal fluctuation of the flapping cycle that is defined as  $\Delta t$  here.

For such a physiologically abnormal state when flight is restrained by a copper wire, there is a possibility that a statistically significant difference from the EMG at free flight. The  $\Delta t$  of peak-to-peak flapping cannot be obtained using the copper wire that perfectly ignore own lift force. The fluctuation of  $\Delta t$  is the time when Ca ions are replenished to the muscle fibers, and this work is considered to be intermittent. It is thus necessary to conduct experiments with free flight.

Using a dc amplification circuit without capacitive coupling as the EMG amplification circuit, we confirmed that the baseline changes at the gear change point of wing flapping.

The lift provided by the wing can be expressed as angular velocity  $\times$  thoracic weight - air resistance - eddy resistance due to turbulence. In future studies, we plan to attach a micro radio transmitter to the moths to gather data on potential energy, kinetic energy, and displacement during free flight for analysis. Such physiological functional evaluations of moths may give insight into damage to insect health due to repeated exposure to multiple agrochemicals and may lead to significant changes in toxicity standards, which are currently based on LD50 values.

## III. METHODS

### 3.1. The Outline of the Biotelemetry System

Hanging a moth by a copper wire and measuring the EMG signal in a restrained state does not replicate the physiological state. If EMGs from moths could be measured during free flight, there is a possibility of obtaining correlations

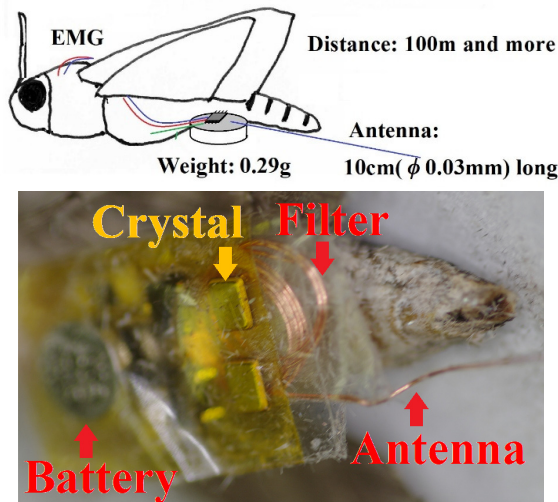


Fig. 5. Concept of the engineering model.

Table 1. List of the parts and weight.

Parts	Weight [g]
Battery	0.1
VCXO	0.08
Microchips	0.05
Solder + copper wire	0.02
Filter+antenna	0.01
Total	0.29

between EMG peak-to-peak fluctuations and lift that could not be obtained in the restrained state. Therefore, we developed a biotelemetry system and measured flight data recorded for approximately 100 m. The average weight of the moths was 1.1 g. Based on empirical data, we considered that an additional 0.28–0.33 g (25%–30% of the moth weight) could be added. The concept of the biotelemetry system is shown in Fig. 5 and the weights of the main components are listed in Table 1.

### 3.2. Block Diagram

The electric potential of the muscle that plays an active part in the flapping of a moth (EMG) was acquired with three electrodes and amplified by a factor of 134 using an operational amplifier. The change in the electric potential is converted into a change in frequency (frequency modulation). Spurious signals are removed with a buffer amplifier and the remaining signals are transmitted at a radio-frequency (RF) power of  $-7\text{dBm}$ . A block diagram of the transmitter is shown in Fig. 6.

### 3.3. Battery and Power Consumption

For the proposed device, the battery capacity is limited to 8 mAh. Therefore, if the current of the bipolar transistor

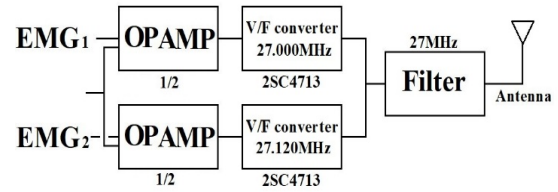


Fig. 6. Block diagram of the transmitter.

(2SC4713) in the final stage of the transmitter is not suppressed, the battery will be exhausted immediately. The transmission power can be adjusted by changing the resistance  $R$  connected to the emitter of the bipolar transistor. A current of approximately 20 mA flows when  $R=35\ \Omega$  and the operation time is about 24 minutes (Fig. 7). The RF maximum output is 1 mW (0 dBm). Table 2 shows the battery (Sony SR416SW) specifications and Table 3 shows compatible batteries manufactured by other companies.

### 3.4. Free Space Path Loss

According to the license requirements, a filter was inserted to suppress spurious signals for a transmission power of 1 mW. The free space path loss is calculated by the following equation. The simulation of free space path loss was performed by MATLAB 2018 on Windows 10 environment.

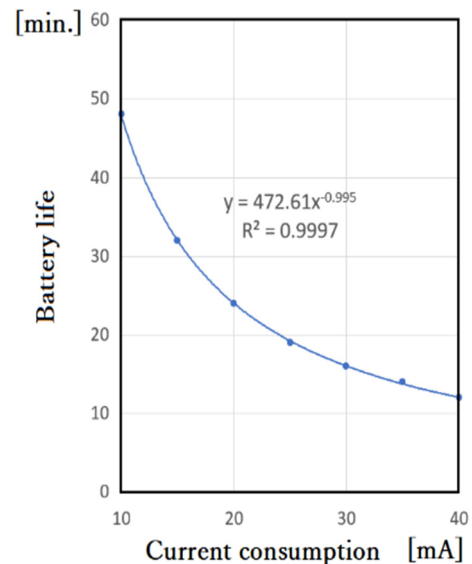


Fig. 7. Current and battery life.

Table 2. Specification of the battery.

Specification	Standard SONY SR416SW
Type	Silver oxide battery
Nominal voltage	1.55 V
Capacity	8 mAh
Size	Diameter 4.8 mm × Height 1.65 mm
Weight	0.1 g

Table 3. Button battery product compatibility.

SONY	SR416SW
ENERGIZER	337
RAYOVAC	337
RENATA	337
BULOVA	623
SEIKO	SB-A5
CITIZEN	280-75
GP	GP337

$FSPL = 20 \times \log(4 \times \pi \times d / \lambda)$   
 $\pi$ : Pai(3.1415)  
 $d$ : Distance (m)  
 $\lambda$ : Wavelength (m) =  $c/f$   
 $c$ : Light speed (m/s)  
 $f$ : Frequency (Hz)

Considering the gain of the transmitting antenna and the gain of the receiving antenna, it can be rewritten as the following Equation (1).

$$FSPL = 20 \log_{10}(d) + 20 \log_{10}(f) + 32.44 - G_t - G_r \quad (1)$$

$G_t$ : Transmitting antenna gain (dB)  
 $G_r$ : Receiving antenna gain (dB)

Because the antenna on a moth is only 10 cm long (diameter: 0.03 mm), efficiency is poor (effective isotropic radiated power: -40 dB). Fig. 8 shows the free space path loss when the receiving side uses a  $1/2\lambda$  dipole antenna. A

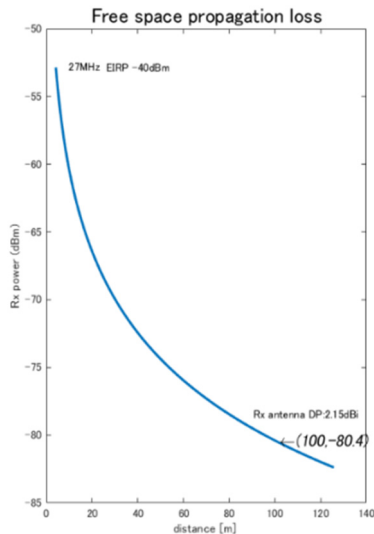


Fig. 8. Free space path loss.

filter must be inserted to suppress spurious signals to -50 dB or less than the main radio wave, as required by law. The bipolar transistor (2SC4713) of the buffer has an amplification ratio of about 8, ensuring an output of 0 dBm (Fig. 8).

### 3.5. Voltage-Frequency Conversion

The EMG of the moth was amplified with the gain of 134 using an operational amplifier (NJU77002RB, JRC) and charged in the variable-capacitance diode of the crystal transmission part. The change in the capacitance of the variable-capacitance diode caused a change in the frequency of the crystal oscillator. This setup is called a voltage-controlled crystal oscillator (VCXO). The relationship between the added control voltage and frequency is shown in Fig. 9. The potential change from 0 to 1.5 V is within the bandwidth of 4 kHz. The relationship between output power and load potential is shown in Fig. 9, Fig. 10 and Fig. 11.

### 3.6. Results of the Experiment

We soldered the devices and components to be mounted on the moth and electrically tested the engineering model before ordering the flexible board. Battery consumption is about 20 minutes if the total current is about 25 mA. The propagation distance is about 100 m, simulated from the

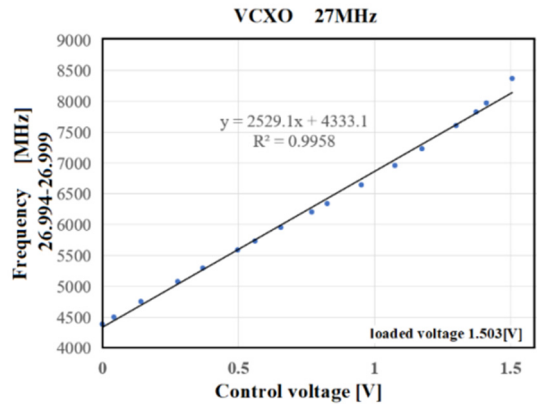


Fig. 9. Relationship between output power and load potential.

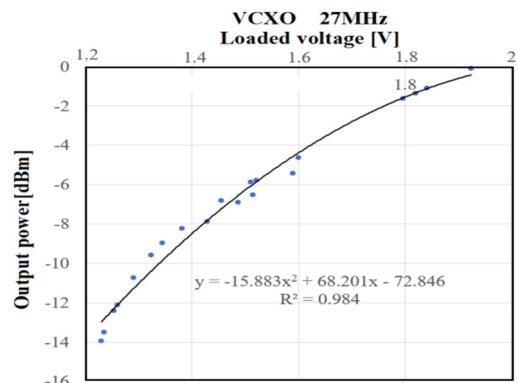


Fig. 10. Loaded voltage and output power of the VCXO.

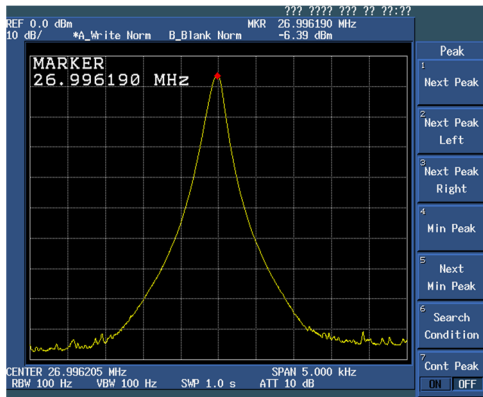


Fig. 11. Monitor of the output power  $-7\text{dBm}$  with spectrum analyzer.

free space path loss equation. The V / F conversion was linear, and the RF, especially the power  $-7\text{ dBm}$ , was stable and satisfactory.

## IV. CONSIDERATIONS

### 4.1. Challenges in Mounting on Flexible Board

Based on the above experimental results, we manufactured a flexible substrate exclusively for hawkmoths, so the points to be noted from design to mounting are described below. For mounting, a flexible substrate with a thickness of  $0.2\text{ mm}$  and double-sided copper foil was used as the preliminary board. In this circuit, most of the back side is the ground, and since it is soldered by hand of a skilled worker in the preliminary stage, sufficient space is taken between the parts for the purpose of distributing heat (Fig. 12) After burning the wiring of the pattern, the time to remove the water from the both layer adhering to the substrate varies depending on the pattern configuration. If the ground is relatively wide like this board, it has a heat dissipation effect, and moisture can be removed by overheating at  $120\text{ C}$  degree for about 30 minutes. It is possible to make it even narrower for small fly. In the future, if it is to be mounted on small moths and butterflies, it would be possible to be narrowed about 64% ( $\text{vertical} \times \text{horizontal} = 4/5 \times 4/5 = 0.64$ ) in size. These conditions reflect the technical level of the laboratory, and if it can be developed commercially, that is, if the budget can be secured, it is desirable to commercialize a dedicated IC as a V/F device (VCXO).

### 4.2. Multi-Functionalization with Limited Weight

Since the weight of the payload has an upper limit of about  $0.28\text{g}$ , we would like to consider carrying two functions with one transistor by the following two methods, and conduct verification experiments in the future. Many papers on techniques for multiplexing with one device and quadrature modulation have been published in the past [23-35].

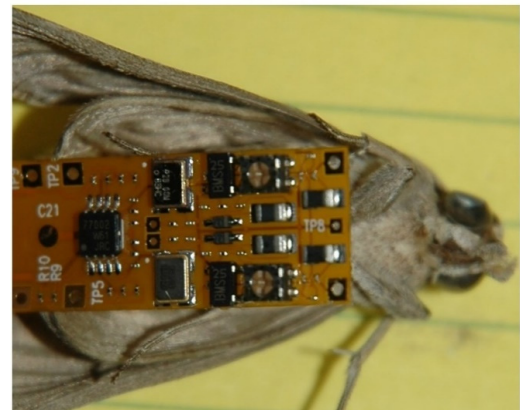
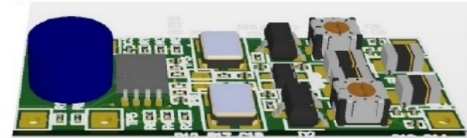
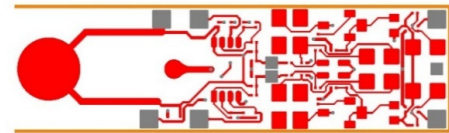


Fig. 12. Upper: Wiring diagram of the prototype board, middle: 3D mockup of parts, lower: Completed flexible board.

#### 4.2.1. Two Channels Via Orthogonalization

Because frequency modulation (FM) is used for the first channel, a second channel can be created using amplitude modulation (AM) on the orthogonal axis. However, the disadvantage is that the signal leaks out during FM demodulation if the frequency component of the AM is high due to the group delay characteristic of the detection of the receiver. The first channel, FM, is suitable for EMG with high-frequency components, and the second channel, AM, is suitable for angular velocity with a relatively slow wave motion.

A dual-gated field-effect transistor (e.g., 3SK284, 3SK73) is used for cascade amplification and resistor  $R_2$  is used to adjust the bias to modulate the Gate-2 voltage from  $-0.1$  to  $-0.4\text{ V}$ . If the signal goes to zero, the FM signal cannot be demodulated. Gate-1 is designed to handle crystal oscillation (Fig. 13 and Fig. 14).

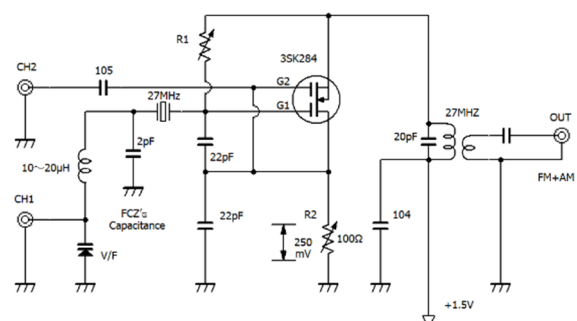


Fig. 13. Idea of orthogonalization modulation with a dual-gated FET.

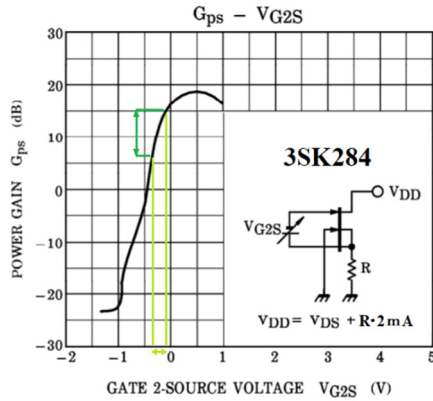


Fig. 14. Suitable voltage for the Gate-2.

#### 4.2.2 Weight Reduction using Reflex System

A system that amplifies two signals with one amplifier circuit is called a reflex system. Such systems have been implemented in middle- or short-wave receivers. A reflex radio amplifies and detects an RF signal and in parallel amplifies an audio frequency (Fig. 15). A single amplification circuit is used for both RF amplification and audio frequency amplification. Based on this concept, a single transistor can be used for the high-frequency crystal oscillation circuit and the low-frequency biological signal amplification. Because the low-frequency amplification cannot achieve a gain of 20 dB, the resolution in the amplitude direction is lower than that of an operational amplifier. As a countermeasure, the capacitance of the varactor diode can be increased, which will expand the frequency band, increase the FM coefficient, and lead to diffusion gain, compensating to a certain degree for the low resolution. Experiments are required to evaluate the implementation.

#### 4.3. Reasons for New Measurement with ICT to Replace LD50

Genetic damage from radiation isotope exposure, sperm, eggs, or immediately after fertilization has been studied. However, we believe that the oxidation of genes in the cells, nucleior mitochondria DNA associated with continuous ex-

posure of low concentrations during the growth process results in a decrease of the function of the living body.

Focusing on the fact that the muscle of Sweetpotato Hornworm is greatly differentiated at the 1st to 3rd instar, low-concentration continuous exposure → cell oxidation → damage to muscle mitochondrial DNA → decrease in ATP in the muscle → decrease in uptake of Ca ions from T tube → Myoelectric potential decreases.

As an experimental model, we think that it is possible to put a radioisotope in the artificial feed of Sweetpotato Hornworm and expose it internally, and measure the flight EMG. We are aiming to find the correlation between the amount of radiation loaded on food and the amplitude of the electromyogram.

LD50, which is an index so far, is an index of the acute phase in which 50% of individuals die, and this is not an index of the chronic phase. In the chronic phase, the value of 1/1000 (for example) of LD50 is simply applied. Anyone can judge which is more scientific.

## V. CONCLUSION

We developed an engineering model of a transmitter for obtaining an EMG of a moth in free flight. From a technical perspective, future development efforts should consider that one element in the reflex system or the cascade method should have multiple functions. If electronic device technology that can quantify EMG during free flight were developed, the detection of physiological abnormalities would allow a physiological standard that replaces the LD50-based standard for continuous low-dose exposure to pesticides and radiation.

## ACKNOWLEDGEMENT

We wish to thank Professor Noriyasu Ando of the Mae-bashi Institute of Technology, who provided the moths used in the present study. We also deeply thank the timely help given by Prof. Kiyoshi Kurokawa, the National Graduate Institute for Policy Studies. This experimental research was assisted by Ms. Miyoshi Tanaka and Ms. Hiroko Ichimura of Nakajima Labo. Tokai University, Ms. Machiko Yoda and Ms. Megumi Amano of Seisa University.

The flexible board of the transmitter was assembled by Japan System Design Inc. Hiroshima City, Japan. The patent included in this research has been applied by Tasada Works Inc. Takaoka City, Japan.

## REFERENCES

[1] K.Sakauchia, W. Tairaab, and A. Hiyam. et al., "The

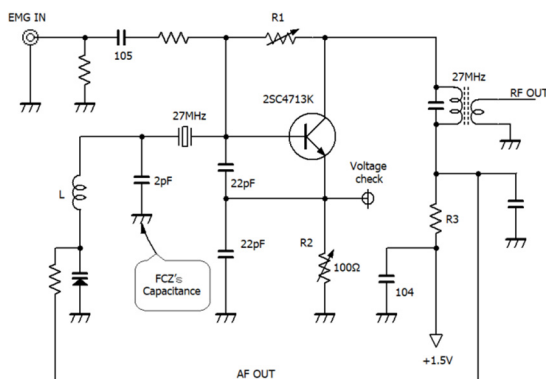


Fig. 15. Idea of the reflex system.

- pale grass blue butterfly in ex-evacuation zones 5.5 years after the Fukushima nuclear accident: Contributions of initial high-dose exposure to transgenerational effects," *Journal of Asia-Pacific Entomology*, vol. 23, no. 1, pp. 242-253, 2020.
- [2] J. Otaki, "Fukushima's lessons from the blue butterfly: A risk assessment of the human living environment in the post-Fukushima era, *Integrated Environmental Assessment and Management*, vol. 12, no. 4, pp. 667-672, 2016.
- [3] J. Otaki and W. Taira, "Current status of the blue butterfly in Fukushima research," *Journal Heredity*, vol. 109, no. 2, pp. 178-187, 2018.
- [4] J. Otaki, A. Hiyama, A., M. Iwata., and T. Kudo, "Phenotypic plasticity in the rangemargin population of the lycaenid butterfly *Zizeeria maha*," *BMC Evolutionary Biology*, vol. 10, no. 1, pp. 252, 2010.
- [5] J. Otaki, Understanding Low-dose exposure and field effects to resolve the field laboratory paradox: Multifaceted biological effects from the Fukushima nuclear accident," in N. S. Awwad, S. A. AlFaify (eds.). *New Trends in Nuclear Science*, London: Intech Open., 2018.
- [6] J. Otaki and W. Taira, "Current status of the blue butterfly in Fukushima research," *Journal of Heredity*, vol. 109, no. 2, pp. 178-187, 2018.
- [7] R. Isenring, Pesticides and the Loss of Biodiversity, Pesticide Action Network Europe, March 2010. [https://www.pan-europe.info/old/Resources/Briefings/Pesticides\\_and\\_the\\_loss\\_of\\_biodiversity.pdf](https://www.pan-europe.info/old/Resources/Briefings/Pesticides_and_the_loss_of_biodiversity.pdf)
- [8] Beyond pesticides, "Impacts of pesticides on wildlife," May 2020, <https://www.beyondpesticides.org/program/s/wildlife>.
- [9] M. DiBartolomeis, S. Kegley, P. Mineau, R. Radford, and K. Klein, "An assessment of acute insecticide toxicity loading (AITL) of chemical pesticides used on agricultural land in the United States," *PLOS-ONE*, vol. 14, no. 8, 2019.
- [10] J. Lundgren and S. Fausti, "Trading biodiversity for pest problems," *Science Advances*, vol. 1, no. 6, Jul. 2015.
- [11] K. Suzuki and T. Inamuro, "An improved lattice kinetic scheme for incompressible viscous fluid flows," *International Journal of Modern Physics C*, vol. 25, no. 1, 2014.
- [12] M. Shindo, T. Fujikawa, and K. Kikuchi, "Analysis of roll rotation mechanism of the butterfly for development of a small flapping robot," in *The 3rd International Conference on Design Engineering and Science (IC DES)*, vol. 3, 2014.
- [13] F. Lehmann and S. Pick, "The aerodynamic benefit of wing-wing interaction depends on stroke trajectory in flapping insect wings," *Journal of Experimental Biology*, vol. 210, no. 8, pp. 1362-1377, 2007.
- [14] S. Hassler, Winged Victory: Fly-Size Wing Flapper Lifts Off," *IEEE Spectrum*, 2008, <https://spectrum.ieee.org/aerospace/aviation/winged-victory-flysize-wing-flapper-lifts-off>
- [15] T. Deora, N. Gundiah, and S. Sane, "Mechanics of the thorax in flies," *Journal of Experimental Biology*, vol. 220, no. 8, pp. 1382-1395, 2017.
- [16] K. Nakada and J. Hata, "Development and physiological assessments of multimedia avian esophageal catheter system," *Journal of Multimedia Information System*, vol. 5, no. 2, pp. 121-130, Jun. 2018.
- [17] I. Nakajima, H. Juzoji, K. Ozaki, and N. Nakamura, "Communications protocol used in the wireless token rings for bird-to-bird," *Journal of Multimedia Information System*, vol. 5, no. 3, pp. 163-170, Sep. 2018.
- [18] K. Nakada, I. Nakajima, J. Hata, and M. Ta, "Study on vibration energy harvesting with small coil for embedded avian multimedia application," *Journal of Multimedia and Information Systems*, vol. 5, no. 1, pp. 47-52, Mar. 2018.
- [19] N. Ando, I. Shimoyama, and R. Kanzaki, "A dual-channel FM transmitter for acquisition of flight muscle activities from the freely flying hawkmoth, *Agrius convolvuli*," *Journal of Neuroscience Methods*, vol. 115, no. 2, pp. 181-187, 2002.
- [20] M. Shimoda, M. Kiuchi, "Oviposition behavior of the sweet potato hornworm, *Agrius convolvuli* (Lepidoptera; Sphingidae), as analysed using an artificial leaf," *Applied Entomology and Zoology*, vol. 33, no. 4. pp. 525-534, 1998.
- [21] A. Zagorinskii, O. Gorbunov, and A. Sidorov, "An experience of rearing some hawk moths (Lepidoptera, Sphingidae) on artificial diets," *Entomological Review*, vol. 93, no. 9, pp. 1107-1115, 2013.
- [22] I. Nakajima and Y. Yagi, "basic physiological research on the wing flapping of the sweet potato hawkmoth using multimedia," *Journal of Multimedia Information System*, vol. 7, no. 2, pp. 189-196, 2020.
- [23] D. Arbet, M. Kováč, V. Stopjaková and M. Potočný, "Voltage-to-frequency converter for ultra-low-voltage applications," in *2019 42nd International Convention on Information and Communication Technology, Electronics and Microelectronics(MIPRO)*, pp. 53-58, 2019.
- [24] Y. Tian, L. Qiao, and G. Qu, "small signal voltage-frequency conversion processing method for SF6 Sensor," in *2021 3rd International Conference on Artificial Intelligence and Advanced Manufacture(AIAM)*, pp. 339-342, 2021.
- [25] D. D. Wentzloff, A. Alghaihab, and J. Im, "Ultra-low power receivers for IoT applications: A review" in *IEEE Custom Integrated Circuits Conference(CICC)*

2020, pp. 1-8, Mar. 2020.

- [26] A. Alghaihab, Y. Shi, J. Breiholz, H. Kim, B. H. Calhoun, and D. D. Wentzloff, "Enhanced interference rejection bluetooth lowenergy back-channel receiver with LO frequency hopping," *IEEE Journal of Solid-State Circuits*, vol. 54, no. 7, pp. 2019-2027, Jul. 2019.
- [27] J. Im, H. Kim, and D. D. Wentzloff, "A 220-  $\mu$ W  $-83$ -dBm 5.8-GHz third-harmonic passive mixer-first LPWUR for IEEE 802.11ba," *IEEE Transactions on Microwave Theory and Techniques*, vol. 67, no. 7, pp. 2537-2545, 2019.
- [28] J. Moody et al., "Interference robust detector-first near-zero power wake-up receiver," *IEEE Journal of Solid-State Circuits*, vol. 54, no. 8, pp. 2149-2162, 2019.
- [29] V. Mangal and P. R. Kinget, "28.1 A 0.42nW 434MHz  $-79.1$ dBm wake-up receiver with a time-domain integrator," in *2019 IEEE International Solid-State Circuits Conference (ISSCC)*, pp. 438-440, 2019.
- [30] V. Mangal and P. R. Kinget, "A  $-80.9$ dBm 450MHz wake-up receiver with code-domain matched filtering using a continuous-time analog correlator," in *2019 IEEE Radio Frequency Integrated Circuits Symposium (RFIC)*, pp. 259-262, 2019.
- [31] R. Liu et al., "An 802.11ba 495 $\mu$ W  $-92.6$ dBm-Sensitivity BlockerTolerant Wake-up Radio Receiver Fully Integrated with Wi-Fi Transceiver," in *2019 IEEE Radio Frequency Integrated Circuits Symposium (RFIC)*, pp. 255-258, 2019.
- [32] A. Kosari, M. Moosavifar, and D. D. Wentzloff, "A 152 $\mu$ W  $-99$ dBm BPSK/16-QAM OFDM Receiver for LPWAN Applications," in *2018 IEEE Asian Solid-State Circuits Conference (A-SSCC)*, pp. 303-306, 2018.
- [33] J. Moody et al., "A  $-106$ dBm 33nW bit-level duty-cycled tuned RF wake-up receiver," in *2019 Symposium on VLSI Circuits*, pp. C86-C87, 2019.
- [34] P. P. Wang and P. P. Mercier, "28.2 A 220 $\mu$ W  $-85$ dBm sensitivity BLE-compliant wake-up receiver achieving  $-60$ dB SIR via single-die multi-channel FBAR-based filtering and a 4-dimensional wake-up signature," in *2019 IEEE International Solid-State Circuits Conference - (ISSCC)*, 2019, pp. 440-442.
- [35] J. Moody and S. M. Bowers, "Triode-mode envelope detectors for near zero power wake-up receivers," In *2019 IEEE MTT-S International Microwave Symposium (IMS)*, pp. 1499-1502, 2019.

## AUTHORS



**Isao Nakajima** He is a specially appointed professor of Seisa University and a visiting professor of Nakajima Labo. at the Dept. of Emergency Medicine and Critical Care, Tokai University School of Medicine. He got the Doctor of Applied Informatics (Ph.D.), Graduate School of Applied Informatics University of Hyogo 2009, and the Doctor of Medicine (Ph.D.), Post Graduate School of Medical Science Tokai University 1988, and the Medical Doctor (M.D.) from Tokai University School of Medicine 1980. He has been aiming to send huge multimedia data from moving ambulance via communications satellite to assist patient's critical condition. A board member of the Pacific Science Congress, a Rapporteur for eHealth of ITU-D SG2.



**Yoshiya Muraki** Professor, SEISA University, Technical Fellow of Fukuda Denshi Co. Ltd. He graduated from Nihon University, College of Industrial Engineering in March 1974. April 1974, he started his professional carrier at Nihon Dengyo Co. Ltd. to design and developed radio communication equipment, such as SSB transceiver. September 1978, he move to the division of medical telemeters at Fukuda Denshi Co. Ltd. He has been in charge of developing and designing wireless telemetry for medical devices for many years. Professor of Tokai University School of Medicine from 2015 to 2019. In this paper, he was in charge of designing V/F conversion and an operational amplifier with extremely low voltage.



**Kokuryo Mitsuhashi** worked at JVC for 17 years and engaged in research and development of electronic devices. He has developed and designed high-frequency analog circuits that generate plasma at semiconductor manufacturing equipment manufacturers and taught these technologies at the University of Tokyo and major semiconductor manufacturing equipment manufacturers.



**Hiroshi Juzoji** He graduated Tokai University School of Medicine in 1986. For years, he has studied on telemedicine & eHealth and developed circuit design and firmware of special equipment for experimental or practical use. He has visited and installed many small satellite earth stations in the Asia and Pacific region to operate Asia Pacific Medical Network via ETS-V in 1992. Concerning about this study on moth wireless telemetry, he has tested wireless output power and stability.



**Yukako Yagi** is at the Digital Pathology Laboratory of the Josie Robertson Surgical Center serves as an incubator to explore, evaluate and develop new technology to advance digital pathology in a clinical setting and actively engage vendors to help improve the technology and develop clinical applicability. Collaborations with clinical departments (e.g., Surgery), Radiology, Medical Physics, and Informatics groups, enhance these assessments and creates opportunities for multidisciplinary applications. She completed her Doctorate in Medical Science at Tokyo Medical University in Japan. She has a broad interest in various aspects of medical science, which include the development and validation of technologies in digital imaging, such as color and image quality calibration, evaluation and optimization, digital staining, 3D imaging, and decision support systems for pathology diagnosis, research and education. Since joining MSK, she has led pioneering work using MicroCT, Whole Slide Imaging (WSI) and Confocal imaging to connect multi-dimensional and multi-modality images (e.g., single-cell to whole-body analysis). She participated in creating image viewers for several imaging modalities and established new.

